PCCP

View Online
Dynamic Article Links

Cite this: *Phys. Chem. Chem. Phys.*, 2011, **13**, 12545–12553

www.rsc.org/pccp

PAPER

Kinetics of thermo-induced micelle-to-vesicle transitions in a catanionic surfactant system investigated by stopped-flow temperature jump†

Jingyan Zhang[ab] **and Shiyong Liu***[b]

Received 12th December 2010, Accepted 13th April 2011
DOI: 10.1039/c0cp02856h

The kinetics of thermo-induced micelle-to-vesicle transitions in a catanionic surfactant system consisting of sodium dodecyl sulfate (SDS) and dodecyltriethylammonium bromide (DEAB) were investigated by the stopped-flow temperature jump technique, which can achieve T-jumps within ~2–3 ms. SDS/DEAB aqueous mixtures ([SDS]/[DEAB] = 2/1, 10 mM) undergo microstructural transitions from cylindrical micelles to vesicles when heated above 33 °C. Upon T-jumps from 20 °C to final temperatures in the range of 25–31 °C, relaxation processes associated with negative amplitudes can be ascribed to the dilution-induced structural rearrangement of cylindrical micelles and to the dissolution of non-equilibrium mixed aggregates. In the final temperature range of 33–43 °C the obtained dynamic traces can be fitted by single exponential functions, revealing one relaxation time (τ) in the range of 82–440 s, which decreases with increasing temperature. This may be ascribed to the transformation of floppy bilayer structures into precursor vesicles followed by further growth into final equilibrium vesicles *via* the exchange and insertion/expulsion of surfactant monomers. In the final temperature range of 45–55 °C, vesicles are predominant. Here T-jump relaxations revealed a distinctly different kinetic behavior. All dynamic traces can only be fitted with double exponential functions, yielding two relaxation times (τ_1 and τ_2), exhibiting a considerable decrease with increasing final temperatures. The fast process (τ_1 ~ 5.2–28.5 s) should be assigned to the formation of non-equilibrium precursor vesicles, and the slow process (τ_2 ~ 188–694 s) should be ascribed to their further growth into final equilibrium vesicles *via* the fusion/fission of precursor vesicles. In contrast, the reverse vesicle-to-micelle transition process induced by a negative T-jump from elevated temperatures to 20 °C occurs quite fast and almost completes within the stopped-flow dead time (~2–3 ms).

Introduction

Amphiphilic molecules possess the ability of self-assembling into a large variety of morphologically different aggregate microstructures, such as spherical and rod-like micelles, vesicles, and lamellar phases.[1–4] In the past decades, considerable attention has been devoted to theoretical and experimental investigations of the phase behavior, equilibrium microstructures, and morphological transitions of these aggregates.[5–12] In the context of small molecule surfactant systems, microstructural transformation between micelles and vesicles can be induced *via* the variation of surfactant concentrations, temperature, pH, and the presence of external additives (salts, surfactants).[13–24]

Thermo-induced micelle-vesicle transitions are particularly interesting due to the non-invasiveness and facile manipulation of temperature variations.[25–34] Though vesicle-to-micelle transitions upon heating are quite typical in some ionic surfactant systems,[33–35] the reverse process, *i.e.*, heating-induced micelle-to-vesicle transition in surfactant systems is quite rare.[27,30,31] Early examples have been reported by Hoffmann *et al.*[36,37] and Blume *et al.*[38] concerning zwitterionic surfactant/cosurfactant mixtures and lipid/ionic surfactant mixtures, respectively. Later on, Huang *et al.*[30,31] reported several examples of thermo-induced sequential micelle-to-vesicle transitions in catanionic surfactant systems. In one particular example, they observed that the cationic–anionic surfactant system of sodium dodecyl sulfate (SDS)/dodecyltriethylammonium bromide (DEAB) exhibits transitions from cylindrical micelles to vesicles upon heating above ~30 °C.[30] At a temperature range of 30–50 °C, the number density of the vesicles continuously grows at the expense of the cylindrical micelles. At even higher temperatures, vesicle aggregates can be observed. Recently, Holyst, Hao, and coworkers[32] reported that the microstructural evolution between micelles and vesicles in salt-free catanionic

[a] *School of Materials and Chemical Engineering, Anhui Key Laboratory of Advanced Building Materials, Anhui University of Architecture, Hefei, Anhui 230022, China*
[b] *CAS Key Laboratory of Soft Matter Chemistry, Department of Polymer Science and Engineering, University of Science and Technology of China, Hefei, Anhui 230026, China. E-mail: sliu@ustc.edu.cn*

† Electronic supplementary information (ESI) available: See DOI: 10.1039/c0cp02856h

surfactant mixtures of tetradecyltrimethylammonium hydroxide (TTAOH) and fatty acid are mainly dependent on surfactant concentrations.

Although the physicochemical properties and evolution of equilibrium microstructures of these thermo-induced transitions between micellar and vesicular phases have been well-characterized, much less is known concerning the kinetics of thermo-induced micelle-to-vesicle transition and the microstructural reorganization under variation of external conditions. It has been well-recognized that understanding the mechanism(s) and kinetics of micelle-to-vesicle transition and the reverse process is not only of fundamental scientific interest, but also plays a vital role in the context of their technological applications. On the one hand, it provides fresh insights into their microstructural stability and offers new approaches for controlling their final microstructures. Moreover, many vesicle systems are not in the thermodynamic equilibrium state and exist as long-lived metastable structures; thus, exploring the kinetic pathways of their formation is crucial. On the other hand, catanionic vesicles have been the subject of extensive experimental and theoretical investigations due to their long-term stability and spontaneous formation from mixed surfactant systems. The versatile physicochemical properties of catanionic vesicles have allowed for several application-related studies, such as the preparation of magnetic nanoparticles[39] and hollow spheres[40] and the formation of polymer-vesicle gels and networks.[41] Furthermore, they have been employed for the encapsulation of probe molecules[42] and pharmaceutical drugs,[43] or as gene delivery nanocarriers.[44] It is worth noting that the stability, and formation/breakdown kinetics of catanionic vesicles are directly correlated with their functional applications.

Previously, vesicle formation kinetics of catanionic systems consisting of sodium octyl sulfate (SOS)/cetyltrimethylammonium bromide (CTAB), SDS/dodecyltrimethylammonium bromide (DTAB), or lecithin/bile salt mixtures were investigated by the stopped-flow technique in combination with time-resolved laser light scattering (LLS) measurements.[12,45] It has been tentatively proposed that the vesicle formation process consists of a series of events: the fastest is associated with the formation of non-equilibrium mixed aggregates, the following two relaxation steps are the formation of loose or "floppy" bilayer structures through the rearrangement of non-equilibrium mixed aggregates and the formation of vesicle precursors, and the rate-determining step is attributed to the formation of final equilibrium vesicles. Most recent developments in elucidating the vesicle formation kinetics have come from instrumental progress, and the combination of small angle neutron scattering (SANS) or small angle X-ray scattering (SAXS) with the stopped-flow technique allows the accurate probing of microstructural evolution processes, especially at the early stage of vesicle formation. In this context, Gradzielski *et al.* and Narayanan *et al.*[46] investigated the kinetics of micelles-to-vesicle transitions upon stopped-flow equimolar mixing of anionic surfactants with cationic or zwitterionic surfactants detected by SAXS. They proposed that the vesicle formation is a complex multistep process: starting with the quick formation of non-equilibrium mixed globular micelles and the subsequent dissolution with a time constant of 0.5–1 s; after or accompanied with the micelle dissolution process, bilayers then quickly form and slowly transform into unilamellar vesicles; the subsequent process is the growth of vesicles into larger and more monodisperse ones.

Another important issue in understanding the vesicle formation kinetics is to elucidate the underlying mechanisms and pathways. The aggregation dynamics of small molecule surfactant near the association equilibrium can be relatively well described by the Aniansson and Wall (A–W) theory with an important assumption that all changes are due to an elementary process of insertion/expulsion of individual chains ('unimers') into/out of the micelle.[47,48] Kahlweit and coworkers[49,50] later proposed that at higher surfactant concentrations, micelle fusion/fission process is favored instead of the unimer insertion/expulsion pathway. Experimental studies in this aspect revealed that both mechanisms might take effect during the vesicle formation process, which is dependent on specific systems.

To the best of our knowledge, the kinetics of thermo-induced micelle-to-vesicle transition has never been investigated in literature reports possibly due to the following two reasons: (1) the lack of appropriate surfactant systems; (2) the lack of suitable instrumental techniques. Existing techniques of temperature jump are typically induced by laser flash or electric discharge, and the temperature elevation can be only maintained up to 10–100 ms, which is surely not long enough for the monitoring of vesicle formation kinetics.[51] Recent technical progress has allowed the design of stopped-flow devices coupled with the millisecond temperature jump (mT-jump) accessory. Thus, temperature jumps can be conveniently achieved with a typical dead time of 2–3 ms. Most importantly, the measurement time windows can be extended up to several hours.[52] Herein, we report the first kinetic investigation of thermo-induced micelle-to-vesicle transition and the reverse process of SDS/DEAB catanionic surfactant system by employing stopped-flow T-jump coupled with light scattering detectors. By controlling the final temperatures, the transformation kinetics from cylindrical micelles to the micelle/vesicle coexisting phase and to the pure vesicular phase has been probed. In combination with the experimental results, we proposed that the thermo-induced vesicle formation pathway strongly depends on the final temperatures. The thermo-induced vesicle-to-micelle transition kinetics and relevant mechanisms were also explored.

Experimental section

Materials

Sodium dodecyl sulfate (SDS) (analytical grade, Shanghai Chemical Reagent Co.) was recrystallized from anhydrous ethanol. Dodecyltriethylammonium bromide (DEAB) was synthesized from dodecyl bromide and triethylamine, and the crude product was recrystallized three times from acetone/ethanol mixtures.[30] Stock solutions of SDS/DEAB mixtures were prepared in deionized water. For stopped-flow studies, all solutions prior to mixing were filtered through 0.45 μm nitrocellulose filters (Acrodisc) to remove dusts.

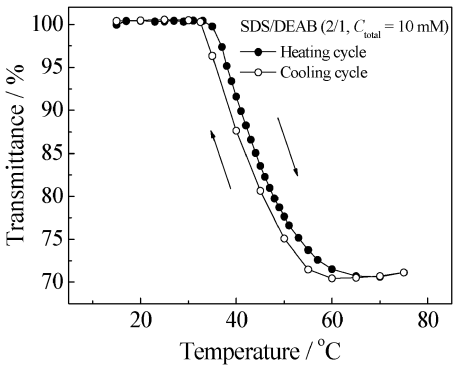

Fig. 1 Temperature-dependent optical transmittance at a wavelength of 600 nm recorded for SDS/DEAB aqueous mixture at [SDS]/[DEAB] = 2 : 1 and a total surfactant concentration of 10 mM.

Transmittance measurements

The optical transmittance of the aqueous solution at a wavelength of 600 nm was acquired on a Unico UV/vis 2802PCS spectrophotometer equipped with a thermostatically controlled cuvette.

Stopped-flow temperature jump with light-scattering detection

Stopped-flow studies were carried out using a Bio-Logic SFM300/S stopped-flow instrument. It is equipped with three 10 mL step-motor-driven syringes (S1, S2, and S3), which can be operated independently to carry out single- or double-mixing. The stopped-flow device is attached to a MOS-250 spectrometer; kinetic data are fitted using the Biokine program provided by Bio-Logic. For the light scattering detection at a scattering angle of 90°, both the excitation and emission wavelengths were adjusted to 335 nm with 10 nm slits. Using FC-08 or FC-15 flow cells, typical dead times are 1.1 ms and 2.6 ms, respectively. All kinetic traces were averaged from at least five consecutive T-jump kinetic measurements.

The millisecond temperature jump (mT-jump) accessory is equipped with a standard Bio-Logic stopped-flow observation cell, which achieves temperature changes by mixing two solutions of different initial temperatures (T_1 and T_2), and the final temperature of the mixture (T_{final}) is determined by the initial temperature (T_1 and T_2) and the mixing ratio. Three thermo-electric Peltier elements are used to control the initial temperatures of the two solutions and that of the observation cell after mixing. The temperature of the mixed solution was calibrated to be the same as the observation cell (Peltier controlled) with the aid of a thermosensitive fluorescent dye, *N*-acetyl-L-tryptophanamide (NATA). The precision of the temperature jump is within ±0.1 °C, and the temperature stability in the observation cell after the temperature jump is <1% in 30 s. For the experimental setup in this work, the T-jump of the SDS/DEAB aqueous mixture ([SDS]/[DEAB] = 2/1, 20 mM) from low to high temperatures (to induce micelle-to-vesicle transition) at an initial temperature of 20 °C (T_1) was achieved by 1 : 1 v/v mixing with water at different temperatures (T_2, 20–90 °C) to target for varying final temperatures (T_{final}, 20–55 °C) and a final concentration of 10 mM. On the other hand, the vesicle-to-micelle transition was induced by T-jump from high to low temperatures for the surfactant mixture ([SDS]/[DEAB] = 2/1, 30 mM) at varying initial temperatures (38–50 °C) by 1 : 2 v/v mixing with cold water (10–22 °C) to target a final temperature of 20 °C and a final concentration of 10 mM.

Results and discussion

Temperature-dependent optical transmittance measurements

Previously, Huang *et al.*[30] systematically investigated thermo-induced micelle-to-vesicle transitions in SDS/DEAB catanionic surfactant systems by employing a combination of dynamic LLS, freeze fracture electron microscopy (FF-EM), and rheological measurements. At 20 °C, they observed that cylindrical micelles are the major aggregates coexisting with a few small spherical vesicles, and the intensity-average hydrodynamic radius, $\langle R_h \rangle$, is ~25 nm. As the temperature increased to ~30 °C, more vesicles are observed ($\langle R_h \rangle$ ~ 100 nm). Further temperature increase is associated with an increase in the number density of vesicles at the expense of cylindrical micelles. At ~40 °C, vesicles are the dominating aggregates, whereas at 50 °C, cylindrical micelles almost completely disappear and a few vesicle aggregates also form. They ascribed the observed thermo-induced micelle-to-vesicle transition to the weakened hydration of surfactant head groups at elevated temperatures.

We measured the temperature dependence of optical transmittance at a wavelength of 600 nm for SDS/DEAB aqueous mixtures at [SDS]/[DEAB] = 2/1 and a total surfactant concentration of 10 mM (Fig. 1). In reasonable agreement with the results reported by Huang *et al.*,[30] we found that heating the aqueous mixture from 15 °C to 33 °C leads to almost no changes in optical transmittance, apparently indicating the lack of any major morphological transformations. Above 33 °C, the optical transmittance abruptly decreases to ~70% at 60 °C, which stabilizes out at even higher temperatures. As reported by Huang *et al.*,[30] this can be ascribed to the micelle-to-vesicle transition. Higher temperatures are advantageous to the formation of vesicles with larger number densities. At a temperature range of 15–75 °C, no macroscopic phase separation can be observed. Fig. 1 also shows temperature-dependent changes of optical transmittance in the cooling cycle, indicating that the micelle-to-vesicle transition is quite reversible in nature.

Kinetics of thermo-induced micelle-to-vesicle transition: T-jump from 20 °C to final temperatures in the range of 25–31 °C

Fig. 2 depicts time-dependent scattered light intensities recorded for an SDS/DEAB aqueous mixture ([SDS]/[DEAB] = 2/1) upon a stopped-flow temperature jump from 20 °C to final temperatures in the range of 25–31 °C. All dynamic traces exhibit an initial decrease and then stabilize out. We can apparently observe that the higher the final temperatures, the slower the kinetic processes. Note that for stopped-flow experiments, the observed kinetics upon T-jump should be ascribed to dynamic processes occurring for the surfactant mixture at 10 mM (final concentration after stopped-flow 1 : 1 v/v mixing) as the uniform physical mixing process (associated with dilution) completes within a millisecond. We also plotted

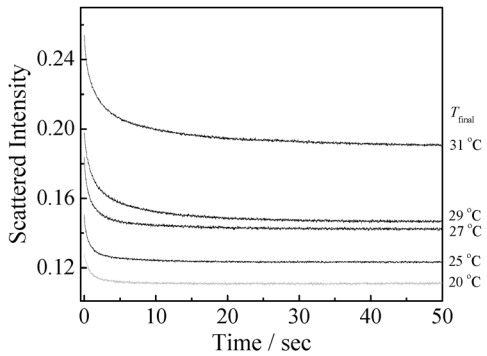

Fig. 2 Time dependence of scattered light intensities recorded for SDS/DEAB aqueous mixture ([SDS]/[DEAB] = 2/1) upon stopped-flow temperature jump from 20 °C to varying final temperatures in the range of 25–31 °C. All temperature jump experiments involve 1 : 1 v/v dilution. Also shown (grey line) is the dynamic trace obtained upon stopped-flow 1 : 1 v/v dilution at 20 °C. The final total surfactant concentration is 10 mM.

the dynamic trace recorded upon stopped-flow 1 : 1 v/v dilution of the aqueous mixture at 20 °C, which shows an initial quick decrease and stabilizes out after ~3–4 s. At 20 °C, cylindrical micelles are the major form of aggregates for SDS/DEAB aqueous mixtures with the total concentration being 10 or 20 mM. Thus, the initial decrease of scattered intensities occurring at 20 °C (*i.e.*, no T-jump) can be ascribed to the dilution effect associated with changes in micellar sizes and the size distributions of cylindrical micelles upon dilution. Previously, we investigated the kinetics of dilution-induced disintegration of worm-like micelles consisting of sodium 4-(8-methacryloyloxyoctyl)-oxybenzene sulfonate (MOBS) and *p*-toluidine hydrochloride (PTHC).[53,54] Initial decrease of scattering intensities upon stopped-flow dilution is also observed at final concentrations much higher than the critical aggregation concentrations (CACs).

Although the relaxation process at other final temperatures associated with negative amplitudes are similar to that occurring at 20 °C, the values of the initial and final equilibrium scattering intensities apparently increase with the final temperatures. The larger scattering intensity at higher final temperatures should be ascribed to the slight increase, although very low, of the number density of spherical vesicles, as suggested by Huang and coworkers[30,31] through dynamic LLS and rheology measurements. The more prominent growth of the initial scattering intensity (*i.e.*, ~2–3 ms after stopped-flow mixing) at higher final temperatures implies that more kinetic events might have occurred in addition to the dilution effects. The initial fast process (which completes within the stopped-flow dead time, ~2–3 ms) associated with the increase in light scattering intensity occurs although we only observed relaxation processes with negative amplitudes. In combination with the results reported by Hatton *et al.*,[45] we tentatively ascribe the initial fast process to the formation of non-equilibrium mixed aggregates, whereas the subsequent decrease in scattering light intensity can be attributed to the dissolution/structural rearrangement of non-equilibrium aggregate structures due to their poor structural stability. This is reasonable considering that within the investigated final temperature range (25–31 °C), cylindrical micelles are the predominant form. We thus established that dynamic traces are a combination of the results of the dilution effects and the initial formation of non-equilibrium mixed aggregates, and their subsequent structural rearrangement.

All the dynamic traces in Fig. 2 can be fitted with single exponential functions. The final temperature dependence of relaxation times is plotted in Fig. 3, which is in the range of ~1.2–2.8 s. We can clearly observe an increase in relaxation times with increasing final temperatures. At elevated temperatures, the higher structural stability of the initially formed non-equilibrium mixed aggregates might lead to longer time scales required for aggregate disintegration and structural rearrangement.

T-jump from 20 °C to final temperatures in the range of 33–43 °C

Upon a stopped-flow temperature jump from 20 °C to final temperatures in the range of 33–43 °C, the time dependence of scattered light intensity recorded for SDS/DEAB aqueous mixture is shown in Fig. 4a. Closer examination of the dynamic trace recorded upon T-jump from 20 °C to 33 °C (Fig. 4b) reveals that the scattered light intensity shows an abrupt decrease within the first ~20 s, and then gradually increases with time even after ~3000 s. As discussed in the previous section, the initial decrease in scattered light intensity should be mainly ascribed to the disintegration of quickly formed non-equilibrium mixed aggregates. Since vesicles starts to appear at final temperatures ≥ 33 °C, it is quite expected that the observed increase in scattered light intensity at later stages should be attributed to the formation of floppy bilayer structures, the subsequent closure into precursor vesicles, and then the vesicle growth.

At these final temperatures, only one relaxation process associated with positive amplitude can be typically observed, and we do not observe any relaxation process associated with negative amplitude. It can be inferred from previous examples that during vesicle formation, the formation of intermediate states (*e.g.*, floppy bilayer structures) is a very fast process (within ~1 s).[46,55] The observed time-dependence of scattered light intensity is drastically different compared to that at a final temperature of 33 °C, which exhibits dramatic and abrupt

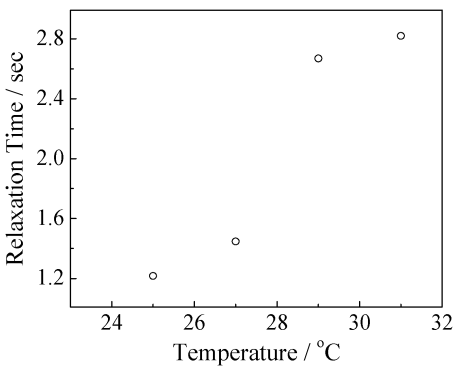

Fig. 3 Final temperature dependence of relaxation times obtained from the single exponential fitting of stopped-flow dynamic traces shown in Fig. 2.

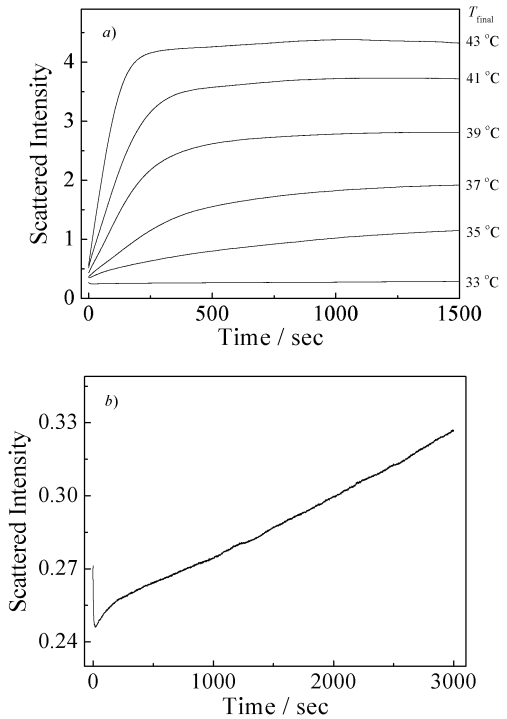

Fig. 4 (a) Time dependence of scattered light intensities obtained for SDS/DEAB aqueous mixture ([SDS]/[DEAB] = 2/1) upon stopped-flow temperature jump from 20 °C to varying final temperatures in the range of 33–43 °C. (b) Dynamic curve obtained upon stopped-flow temperature jump from 20 to 33 °C with extended time windows (0–3000 s). All temperature jump experiments involve 1 : 1 v/v dilution. The final total surfactant concentration is 10 mM.

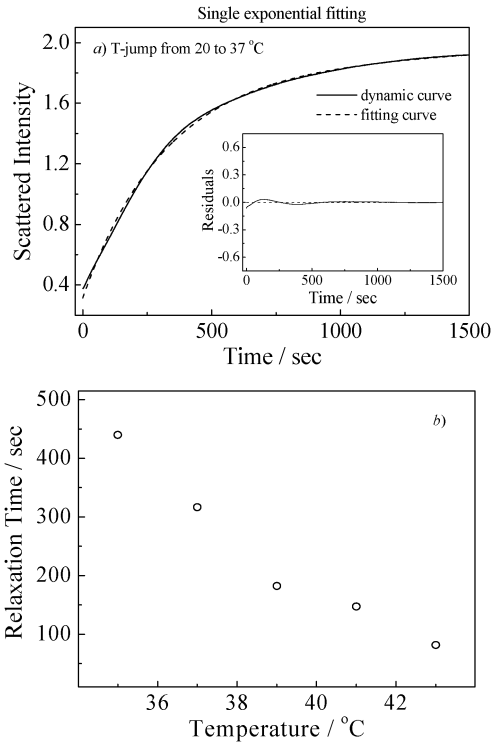

Fig. 5 (a) Typical time dependence of scattered light intensity of SDS/DEAB mixed aqueous solution recorded upon stopped-flow temperature jump from 20 to 37 °C. Also shown is the single exponential fitting curve. (b) Single exponential fitting results of dynamic traces shown in Fig. 4a.

changes in scattered light intensity. Moreover, the final scattered intensities increase with final temperatures, suggesting an increase in the number density of the aggregates (cylindrical micelles and vesicles). It should be noted that at a final temperature range of 33–43 °C, vesicles are not the dominating morphology and most of the aggregates exist in the form of cylindrical micelles.

The time dependence of scattered light intensity I_t can be converted to a normalized function, namely, $(I_\infty - I_t)/I_\infty$ *versus* t, where I_∞ is the value of I_t at an infinitely long time. All dynamic traces at the final temperature range of 35–43 °C in Fig. 4a can be fitted with a single exponential function:

$$(I_\infty - I_t)/I_\infty = ce^{-t/\tau} \quad (1)$$

where c is the normalized amplitude, τ is the relaxation time associated with a specific kinetic process. Fig. 5a shows a typical fit of the dynamic trace upon stopped-flow T-jump from 20 °C to 37 °C, resulting in a relaxation time, τ, of 315 s. The quality of the fit is assessed from the reduced χ^2 error values, which is defined by

$$\chi^2 = \frac{1}{N}\sum_{i=1}^{n}(x_i - \bar{x}_i)^2$$

where N, x_i, and $\bar{x}_i$ are the number of data points, and values of the experimental data and fitting data, respectively. For a temperature jump from 20 °C to 37 °C, the χ^2 error value for the single-exponential fitting is 0.49, and a double-exponential fitting was also tested. The fitting was not significantly improved *via* the introduction of the second exponential expression as χ^2 decreased only by 15%. The single exponential fitting results of dynamic traces recorded at final temperatures in the range of 35–43 °C are plotted in Fig. 5b. Apparently, the formation of final vesicles is much faster at higher final temperatures. The obtained relaxation times vary in the range of 82–440 s, which decrease dramatically with increasing temperatures.

T-jump from 20 °C to final temperatures in the range of 45–55 °C

Upon jumping from 20 °C to final temperatures in the range of 45–55 °C, relaxation processes with quite large positive amplitudes are observed. Fig. 6 shows the time dependence of scattered light intensity obtained for SDS/DEAB aqueous mixture upon stopped-flow temperature jump from 20 °C to the final temperature range of 45–55 °C. It seems that the final scattered light intensities remain nearly constant upon further heating. Fig. 7 shows the final temperature dependence of the scattered light intensity recorded upon a stopped-flow temperature jump from 20 °C to varying final temperatures in the range of 33–55 °C. The final scattered light intensity continuously increases up to 45 °C and then stabilizes out. Above 45 °C, cylindrical micelles completely transform into vesicles, which is the dominant morphology.

It is worth noting that in Fig. 7, the final scattering intensity upon T-jump remains almost constant above ~45 °C, whereas in Fig. 1 the optical transmittance is still decreasing above

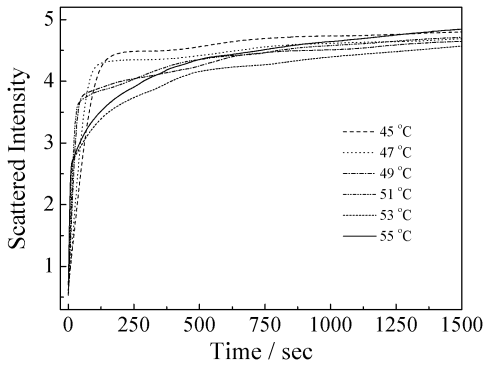

Fig. 6 Time dependence of scattered light intensities obtained for SDS/DEAB mixed aqueous solutions ([SDS]/[DEAB] = 2/1) upon a stopped-flow temperature jump from 20 °C to varying final temperatures in the range of 45–55 °C. All temperature jump experiments involve 1 : 1 v/v dilution. The final total surfactant concentration is 10 mM.

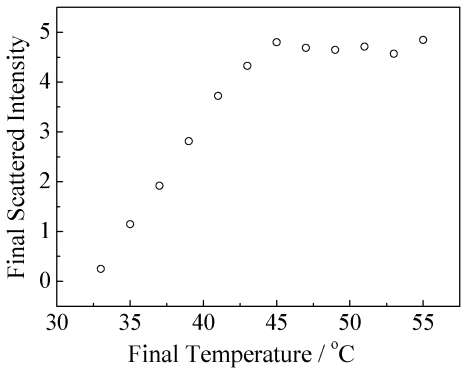

Fig. 7 Final temperature dependence of scattered light intensities for SDS/DEAB mixed aqueous solutions ([SDS]/[DEAB] = 2/1) recorded 1500 s after a stopped-flow temperature jump from 20 °C to varying final temperatures in the range of 33–55 °C. The final total surfactant concentration is 10 mM.

45 °C. As for the observed apparent discrepancy, we tentatively interpret it as follows: (1) all kinetic data shown in Fig. 7 results from a T-jump from 20 °C to varying final temperatures (45–55 °C), the fast T-jump (within a millisecond) results in different kinetic pathways towards the formation of vesicles as compared to the slow heating rate; whereas in Fig. 1, the temperature is gradually increasing and at every temperature point ~20 min is required for the thermal equilibration. Thus, the different thermal history during the micelle-to-vesicle transition should contribute to the observed discrepancy in final scattering intensities; (2) for the kinetic data shown in Fig. 6, the measuring time window is 0–1500 s; note that the scattering intensity is still further increasing at extended time periods during the process forming final equilibrium vesicles, and sometimes, this process might take a few days or weeks.

Single- and double-exponential fitting results of dynamic traces upon stopped-flow T-jump from 20 °C to 55 °C are shown in Fig. 8. It is found that the single exponential function cannot fit the relaxation curve very well (Fig. 8a), especially for the first 10 s; the associated χ^2 error is ~17.6. However, the dynamic trace can be fitted by a double exponential function (Fig. 8b, eqn (2)), resulting in a prominent improvement of χ^2 of 0.61:

$$(I_\infty - I_t)/I_\infty = c_1 e^{-t/\tau_1} + c_2 e^{-t/\tau_2} \quad (2)$$

where c_1 and c_2 are the normalized amplitudes ($c_2 = 1 - c_1$), τ_1 and τ_2 are the relaxation times for two processes, $\tau_1 < \tau_2$. The mean relaxation time for the overall micelle formation, τ_f, can be calculated as

$$\tau_f = c_1\tau_1 + c_2\tau_2 \quad (3)$$

Both processes associated with τ_1 and τ_2 possess positive amplitudes. For a stopped-flow temperature jump experiment from 20 °C to 55 °C, τ_1 and τ_2 are approximately 5.2 s and 188 s, respectively. The calculated τ_f based on eqn (3) is ~73 s. The fitting results are summarized in Table S1 in the ESI.†

Fig. 9 shows the double exponential fitting results of dynamic traces in Fig. 6. The relaxation time, τ_1, is in the range of 5.2–28.5 s, and decreases with increasing temperatures; τ_2 ranges from 188 to 694 s, and also decreases with increasing temperatures. The calculated τ_f based on eqn (3) is in the range of 73–162 s. We can apparently judge that the higher the final temperatures, the faster the growth rate of the aggregates. On the other hand, the amplitudes associated with the two processes, c_1 and c_2, exhibit distinctly different final temperature dependences, with the former (c_1, 0.58–0.88) decreasing with increasing temperatures, and the latter c_2 (0.12–0.42) increasing with an increase in the final temperatures.

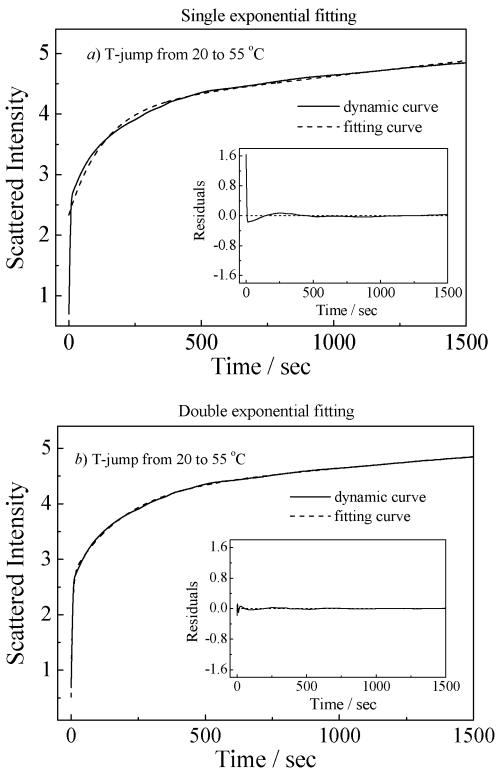

Fig. 8 (a) Single and (b) double exponential fitting results of the dynamic trace recorded for SDS/DEAB aqueous mixture ([SDS]/[DEAB] = 2/1) upon stopped-flow temperature jump from 20 to 55 °C. The final total surfactant concentration is 10 mM.

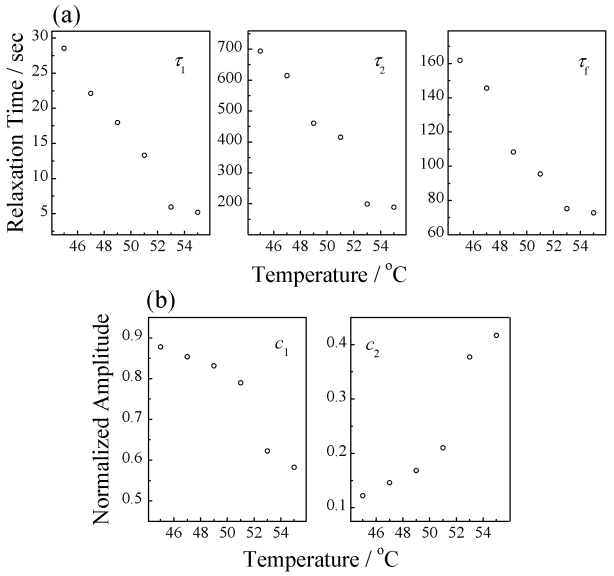

Fig. 9 Double exponential fitting results of dynamic traces obtained upon stopped-flow temperature jump from 20 °C to varying final temperatures in the range of 45–55 °C. The experimental conditions are the same as those described in Fig. 6.

Thermo-induced micelle-to-vesicle transition mechanisms

The thermo-induced morphological transformation between micelles and vesicles in SDS/DEAB mixed surfactant solutions can be explained by the well-known theory of the packing parameter p, proposed by Mitchell *et al.* and Israelachvili *et al.*:[56] $0 \leq p \leq 1/3$ for spherical micelles, $1/3 \leq p \leq 1/2$ for cylindrical micelles, and $1/2 \leq p \leq 1$ for bilayer structures (p is defined as v/a_0l_c, where v is the surfactant tail volume, l_c is the tail length, and a_0 is the equilibrium area per molecule at the aggregate surface). With the increase of temperatures, it is expected that the hydration of surfactant ionic head groups are progressively weakened, hence, the surface area of the micelle per surfactant ion occupied (a_0) is reduced. Correspondingly, an increase in the packing parameter p then leads to the formation of larger aggregates such as cylindrical micelles and vesicles.

Recent theoretical considerations and experimental results concerning the vesicle formation kinetics have established that the micelle-to-vesicle transition typically involves a series of kinetic steps: rapid formation of non-equilibrium mixed aggregates and floppy bilayer intermediates, growth of disk-like micelles and their enclosure into vesicle precursors, and the formation of final equilibrium vesicles.[9,11,17,20,23,45,46,55,57,58] Based on the experimental results presented in Fig. 2–9, we can judge that the kinetic process of micelle-to-vesicle transition in the SDS/DEAB system is highly temperature dependent. At final temperatures below 31 °C, cylindrical micelles are the dominant morphology and the observed kinetics should be ascribed to the structural rearrangement of cylindrical micelles. At final temperatures higher than 31 °C, vesicles start to form. As kinetic events such as the formation of non-equilibrium mixed aggregates and floppy bilayer intermediate structures occur very fast, we can only observe kinetic events at later stages such as the formation of precursor vesicles and final equilibrium vesicles. Our experimental results indicate that upon T-jump from 20 °C to final temperatures in the range of 35–55 °C, the vesicle formation kinetics follow different pathways.

According to theoretical considerations concerning the micellization dynamics of small molecule surfactants, as proposed by Aniansson *et al.*[47,48,59] and Kahlweit *et al.*,[49,50] two mechanisms might be involved in the process of vesicle formation.[60,61] The first one is the gradual addition and exchange of surfactant unimers into/between existing aggregates, and the second mechanism is fusion/fission of small aggregates into final vesicular structures. The fitting results of dynamic traces obtained at different final temperatures can be employed to differentiate between the two possible underlying mechanisms.

Upon T-jump from 20 °C to the final temperature range of 35–43 °C, single-exponential function can fit the relaxation curves. The obtained relaxation time (τ) can be assigned to the transition from floppy bilayer structures into precursor vesicles, accompanied with their further growth into final equilibrium vesicles. Considering the relatively low number density of precursor vesicles, we speculate that the formation of final equilibrium vesicles mainly proceeds *via* the exchange and insertion/expulsion of surfactant monomers.[47,48,60–63]

A closer examination of kinetic traces shown in Fig. 6 can reveal that all kinetic traces recorded upon T-jump from 20 °C to the final temperature range of 45–55 °C apparently exhibit two-stage characteristics, *i.e.*, the initial fast increase in scattering intensity followed by the subsequent much slower process. All relaxation curves can be fitted with double-exponential functions. This is drastically different to those occurring at lower final temperatures (35–43 °C). We ascribe the fast process ($\tau_1 \sim 5.2$–28.5 s) to the formation of non-equilibrium precursor vesicles, and the slow process ($\tau_2 \sim 188$–694 s) to their further growth into final equilibrium vesicles. Both relaxation times, τ_1 and τ_2, exhibit a considerable decrease with an increase of final temperatures (Fig. 9). As for the relaxation process associated with τ_1, we further plotted the temperature-dependence of τ and τ_1 at a final temperature range of 35–55 °C (Fig. S1†). To our surprise, all the data points constitute into a smooth transition curve, which continuously decreases with increasing final temperatures. This further supports the theory that the kinetic process associated with τ_1 in the range of 45–55 °C is of similar origin to that associated with τ in the final temperature range of 35–43 °C.

In general, the slow relaxation process (τ_2), the rate-determining step, can occur *via* the vesicle fusion/fission mechanism or unimer insertion/expulsion mechanism. In the final temperature range of 45–55 °C, all cylindrical micelles transform into vesicles, accompanied with a considerable increase in the number density of vesicles and the formation of vesicle aggregates. Thus, we propose that the slow process (τ_2) should proceed *via* vesicle fusion/fission.[49,50,60,61,64–66] This is in agreement with the fact reported by Huang *et al.*,[30] who revealed that above 50 °C they can clearly observe the presence of vesicle aggregates with dimensions in the range of 200–300 nm. More intriguingly, we found that the amplitudes, c_1 and c_2 (associated with τ_1 and τ_2), exhibit different temperature dependences, with the former decreasing

and the latter increasing with final temperatures. The above analysis indicates that the vesicle formation pathways are highly dependant on the final temperatures. Below and above the critical temperature of 45 °C, the vesicle growth transforms from the unimer insertion/expulsion mechanism to the fusion/fission mechanism. Theoretically, the detailed vesicle growth mechanism can be differentiated *via* the concentration dependences of associated relaxation times,[53,54,67–70] however, in the current case, the critical micelle-to-vesicle transition temperature varies dramatically with the total surfactant concentrations.

Kinetics of thermo-induced vesicle-to-micelle transition

The temperature dependent optical transmittance measurements shown in Fig. 1 suggest that upon cooling, the SDS/DEAB aqueous mixture exhibits the reverse vesicle-to-micelle transition. We further employed the stopped-flow T-jump technique to investigate the associated kinetic processes. It should be noted that the samples for the investigation of vesicle-to-micelle transition kinetics were subjected to ~15 days storage prior to the measurements, allowing them to reach the final equilibrium. Fig. 10 shows the time dependence of scattered light intensities recorded for the SDS/DEAB aqueous mixture upon stopped-flow T-jump from varying initial temperatures (50 °C, 45 °C, and 38 °C) to 20 °C. All kinetic studies are associated with 1/2 v/v dilutions with the final total surfactant concentration being 10 mM. The grey line is a dynamic trace obtained upon a stopped-flow 1 : 2 v/v dilution at 50 °C, which exhibits an almost straight line. This indicates that no apparent micro-structural changes can be discerned with the stopped-flow technique within the 1/2 v/v dilution process.

Upon a temperature jump from 50, 45, 38 °C to 20 °C, again, almost straight lines with much lower scattered intensities compared to that at 50 °C are observed. These results reveal that the reverse vesicle-to-micelle transition process is extremely rapid, and that most of the kinetic events complete within the stopped-flow dead time (a few milliseconds). However, a closer examination of the dynamic traces (see inset in Fig. 10) still reveals the decrease of scattered light intensities, though quite small, within the time window of 0–800 s. The observed decrease in scattered intensity should be ascribed to the later stage during the process of thermo-induced transition from vesicles to cylindrical micelles. Within the stopped-flow dead time, all vesicles quickly disintegrate into small aggregates, and the subsequent slow process with relaxation time in the order of a few hundred seconds is associated with the structural rearrangement of small aggregates into cylindrical micelles.

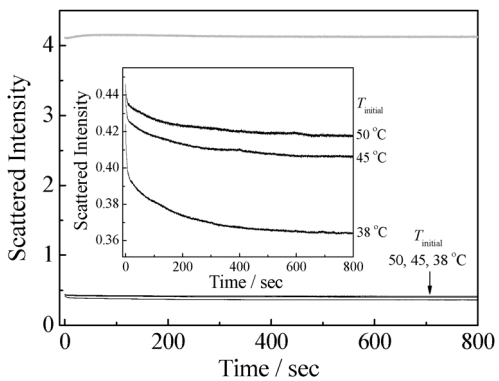

Fig. 10 Time dependence of scattered light intensities recorded for SDS/DEAB aqueous mixtures ([SDS]/[DEAB] = 2/1) upon stopped-flow temperature jump from varying initial temperatures (50, 45, and 38 °C) to 20 °C. All temperature jump experiments involve 1 : 2 v/v dilution. The grey line is a dynamic trace obtained upon 1 : 2 v/v stopped flow dilution at 50 °C. The final total surfactant concentration is 10 mM.

Conclusions

The stopped-flow temperature jump technique was applied to probe the kinetics of thermo-induced micelle-to-vesicle and vesicle-to-micelle transitions in the SDS/DEAB catanionic surfactant system. The obtained temporal variations in scattered light intensities during microstructural changes were employed to elucidate the underlying transition mechanism. We conclude that kinetic sequences associated with the thermo-induced micelle-to-vesicle transition are highly dependant on the final temperatures. If the final temperature is in the range of 33–43 °C, the obtained dynamic traces can be fitted by single exponential functions, and the obtained relaxation times (τ) decrease with an increase in the final temperatures. We tentatively ascribe this process to the transformation of floppy bilayer structures (which quickly form upon T-jumps) into precursor vesicles, accompanied with their further growth into final equilibrium vesicles. Considering the relatively low number density of precursor vesicles, the vesicle growth process should mainly proceed *via* the exchange and insertion/expulsion of surfactant monomers. In the final temperature range of 45–55 °C, vesicles are the predominant morphology. All dynamic traces can only be fitted with double exponential functions, yielding two relaxation times (τ_1 and τ_2), which again exhibit a considerable decrease with an increase of the final temperatures. The fast process should be attributed to the formation of non-equilibrium precursor vesicles, and the slow process is associated with their further growth into final equilibrium vesicles *via* the fusion/fission mechanism. On the other hand, the reverse vesicle-to-micelle transition process induced by stopped-flow T-jump from elevated temperatures to 20 °C occurs quite fast and most of the kinetic events complete within the stopped-flow dead time (~2–3 ms). We can only discern a slow relaxation process (with the relaxation time on the order of a few hundred seconds) at the later stage of thermo-induced vesicle-to-micelle transition.

Acknowledgements

The financial support of the National Natural Scientific Foundation of China (NNSFC) Projects (20874092, 51033005, 21004001, and 91027026), Fundamental Research Funds for the Central Universities, and Specialized Research Fund for the Doctoral Program of Higher Education (SRFDP) is gratefully acknowledged.

Notes and references

1 V. Degiorgio and M. Corti, *Physics of Amphiphiles: Micelles, Vesicles and Microemulsions*, North Holland, Amsterdam, 1985.
2 B. Jonsson, B. Lindman, K. Holmberg and B. Kronberg, *Surfactants and Polymers in Aqueous Solutions*, Wiley, New York, 1998.
3 D. F. Evans and H. Wennerstrom, *The Colloidal Domain: Where Physics, Chemistry, Biology, and Technology Meet*, VCH Publishers, New York, 1994.
4 R. Zana, *Surfactant Solutions: New Methods of Investigation*, Marcel Dekker, New York, 1987.
5 H. Wennerstrom and B. Lindman, *Phys. Rep-Rev. Sec. Phys. Lett.*, 1979, **52**, 1–86.
6 Y. Chevalier and T. Zemb, *Rep. Prog. Phys.*, 1990, **53**, 279–371.
7 Y. Chevalier, *Curr. Opin. Colloid Interface Sci.*, 2002, **7**, 3–11.
8 M. J. Lawrence, *Chem. Soc. Rev.*, 1994, **23**, 417–424.
9 M. Gradzielski, *Curr. Opin. Colloid Interface Sci.*, 2004, **9**, 256–263.
10 A. Khan, *Curr. Opin. Colloid Interface Sci.*, 1996, **1**, 614–623.
11 M. Gradzielski, *Curr. Opin. Colloid Interface Sci.*, 2003, **8**, 337–345.
12 A. Shioi and T. A. Hatton, *Langmuir*, 2002, **18**, 7341–7348.
13 J. Hao, H. Hoffmann and K. Horbaschek, *J. Phys. Chem. B*, 2000, **104**, 10144–10153.
14 P. A. Hassan, S. R. Raghavan and E. W. Kaler, *Langmuir*, 2002, **18**, 2543–2548.
15 M. Mao, J. Huang, B. Zhu and J. Ye, *J. Phys. Chem. B*, 2002, **106**, 219–225.
16 S. U. Egelhaaf, *Curr. Opin. Colloid Interface Sci.*, 1998, **3**, 608–613.
17 M. Gradzielski, *J. Phys.: Condens. Matter*, 2003, **15**, R655–R697.
18 H. Kashiwagi and M. Ueno, *J. Pharmaceu. Soc. Japan*, 2008, **128**, 669–680.
19 M. M. Kozlov and D. Andelman, *Curr. Opin. Colloid Interface Sci.*, 1996, **1**, 362–366.
20 J. Leng, S. U. Egelhaaf and M. E. Cates, *Biophys. J.*, 2003, **85**, 1624–1646.
21 S. Svenson, *Curr. Opin. Colloid Interface Sci.*, 2004, **9**, 201–212.
22 A. Walter, G. Kuehl, K. Barnes and G. VanderWaerdt, *Biochim. Biophys. Acta, Biomembr.*, 2000, **1508**, 20–33.
23 Y. Xia, I. Goldmints, P. W. Johnson, T. A. Hatton and A. Bose, *Langmuir*, 2002, **18**, 3822–3828.
24 B. Michels and G. Waton, *J. Phys. Chem. B*, 2000, **104**, 228–232.
25 R. Bott, T. Wolff and K. Zierold, *Langmuir*, 2002, **18**, 2004–2012.
26 S. Forster and T. Plantenberg, *Angew. Chem., Int. Ed.*, 2002, **41**, 689–714.
27 N. Gorski and J. Kalus, *Langmuir*, 2001, **17**, 4211–4215.
28 S. Kumar, D. Sharma, Z. A. Khan and D. Kabir ud, *Langmuir*, 2001, **17**, 5813–5816.
29 H. Yin, M. Mao, J. Huang and H. Fu, *Langmuir*, 2002, **18**, 9198–9203.
30 H. Q. Yin, Z. K. Zhou, J. B. Huang, R. Zheng and Y. Y. Zhang, *Angew. Chem., Int.Ed.*, 2003, **42**, 2188–2191.
31 H. Yin, J. Huang, Y. Lin, Y. Zhang, S. Qiu and J. Ye, *J. Phys. Chem. B*, 2005, **109**, 4104–4110.
32 H. Li, S. A. Wieczorek, X. Xin, T. Kalwarczyk, N. Ziebacz, T. Szymborski, R. Holyst, J. Hao, E. Gorecka and D. Pociecha, *Langmuir*, 2010, **26**, 34–40.
33 R. T. Buwalda, M. C. A. Stuart and J. B. F. N. Engberts, *Langmuir*, 2000, **16**, 6780–6786.
34 P. A. Hassan, B. S. Valaulikar, C. Manohar, F. Kern, L. Bourdieu and S. J. Candau, *Langmuir*, 1996, **12**, 4350–4357.
35 E. Mendes, R. Oda, C. Manohar and J. Narayanan, *J. Phys. Chem. B*, 1998, **102**, 338–343.
36 G. Wanka, H. Hoffmann and W. Ulbricht, *Colloid Polym. Sci.*, 1990, **268**, 101–117.
37 H. Hoffmann, K. Horbaschek and F. Witte, *J. Colloid Interface Sci.*, 2001, **235**, 33–45.
38 P. R. Majhi and A. Blume, *J. Phys. Chem. B*, 2002, **106**, 10753–10763.
39 I. I. Yaacob, A. C. Nunes and A. Bose, *J. Colloid Interface Sci.*, 1995, **171**, 73–84.
40 M. Kepczynski, J. Lewandowska, M. Romek, S. Zapotoczny, F. Ganachaud and M. Nowakowska, *Langmuir*, 2007, **23**, 7314–7320.
41 F. E. Antunes, R. O. Brito, E. F. Marques, B. Lindman and M. Miguel, *J. Phys. Chem. B*, 2007, **111**, 116–123.
42 A. Fischer, M. Hebrant and C. Tondre, *J. Colloid Interface Sci.*, 2002, **248**, 163–168.
43 E. J. Danoff, X. Wang, S.-H. Tung, N. A. Sinkov, A. M. Kemme, S. R. Raghavan and D. S. English, *Langmuir*, 2007, **23**, 8965–8971.
44 M. Rosa, M. D. Miguel and B. Lindman, *J. Colloid Interface Sci.*, 2007, **312**, 87–97.
45 A. J. O'Connor, T. A. Hatton and A. Bose, *Langmuir*, 1997, **13**, 6931–6940.
46 S. Schmolzer, D. Grabner, M. Gradzielski and T. Narayanan, *Phys. Rev. Lett.*, 2002, **88**, 258301.
47 E. A. G. Aniansson and S. N. Wall, *J. Phys. Chem.*, 1975, **79**, 857–858.
48 E. A. G. Aniansson, S. N. Wall, M. Almgren, H. Hoffmann, I. Kielmann, W. Ulbricht, R. Zana, J. Lang and C. Tondre, *J. Phys. Chem.*, 1976, **80**, 905–922.
49 M. Kahlweit, *J. Colloid Interface Sci.*, 1982, **90**, 92–99.
50 E. Lessner, M. Teubner and M. Kahlweit, *J. Phys. Chem.*, 1981, **85**, 1529–1536.
51 A. Patist, J. R. Kanicky, P. K. Shukla and D. O. Shah, *J. Colloid Interface Sci.*, 2002, **245**, 1–15.
52 Y. F. Zhang, T. Wu and S. Y. Liu, *Macromol. Chem. Phys.*, 2007, **208**, 2492–2501.
53 Z. Y. Zhu, Y. I. Gonzalez, H. X. Xu, E. W. Kaler and S. Y. Liu, *Langmuir*, 2006, **22**, 949–955.
54 Z. Y. Zhu, H. X. Xu, H. W. Liu, Y. I. Gonzalez, E. W. Kaler and S. Y. Liu, *J. Phys. Chem. B*, 2006, **110**, 16309–16317.
55 S. U. Egelhaaf and P. Schurtenberger, *Phys. Rev. Lett.*, 1999, **82**, 2804–2807.
56 J. N. Israelachvili, D. J. Mitchell and B. W. Ninham, *J. Chem. Soc., Faraday Trans*, 1976, **2**, 1525.
57 S. U. Egelhaaf and P. Schurtenberger, *Phys. B*, 1997, **234–236**, 276–278.
58 T. M. Weiss, T. Narayanan and M. Gradzielski, *Langmuir*, 2008, **24**, 3759–3766.
59 E. A. G. Aniansson and S. N. Wall, *J. Phys. Chem.*, 1974, **78**, 1024–1032.
60 S. E. Campbell, H. Yang, R. Patel, S. E. Friberg and P. A. Aikens, *Colloid Polym. Sci.*, 1997, **275**, 303–306.
61 S. E. Campbell, Z. Q. Zhang, S. E. Friberg and R. Patel, *Langmuir*, 1998, **14**, 590–594.
62 I. A. Nyrkova and A. N. Semenov, *Macromol. Theory Simul.*, 2005, **14**, 569–585.
63 I. A. Nyrkova and A. N. Semenov, *Faraday Discuss.*, 2005, **128**, 113–127.
64 F. J. Esselink, E. E. Dormidontova and G. Hadziioannou, *Macromolecules*, 1998, **31**, 4873–4878.
65 F. J. Esselink, E. Dormidontova and G. Hadziioannou, *Macromolecules*, 1998, **31**, 2925–2932.
66 E. E. Dormidontova, *Macromolecules*, 1999, **32**, 7630–7644.
67 Z. Y. Zhu, S. P. Armes and S. Y. Liu, *Macromolecules*, 2005, **38**, 9803–9812.
68 J. Y. Zhang, Z. S. Ge, X. Z. Jiang, P. A. Hassan and S. Y. Liu, *J. Colloid Interface Sci.*, 2007, **316**, 796–802.
69 J. Y. Zhang, J. Xu and S. Y. Liu, *J. Phys. Chem. B*, 2008, **112**, 11284–11291.
70 D. Wang, J. Yin, Z. Y. Zhu, Z. S. Ge, H. W. Liu, S. P. Armes and S. Y. Liu, *Macromolecules*, 2006, **39**, 7378–7385.